Finite size effects in the Kitaev honeycomb lattice model on a torus

Journal of Statistical Mechanics: Theory and Experiment
An IOP and SISSA journal

Finite size effects in the Kitaev honeycomb lattice model on a torus

G Kells, N Moran and J Vala

Department of Mathematical Physics, National University of Ireland, Maynooth, Republic of Ireland
E-mail: gkells@thphys.nuim.ie, nmoran@thphys.nuim.ie and jiri.vala@nuim.ie

Received 14 November 2008
Accepted 15 December 2008
Published 4 March 2009

Online at stacks.iop.org/JSTAT/2009/P03006
doi:10.1088/1742-5468/2009/03/P03006

Abstract. We analyze low energy spectral properties of small toroidal configurations of the Kitaev honeycomb spin model in the Abelian topological phase. We begin with a brief classification of honeycomb lattices on a torus. Then, using the Brillouin–Wigner perturbation theory, we explain the low order finite size effects that can occur in these systems and show how they affect their ground state topological degeneracy. Finally, we demonstrate the accuracy of the perturbative method by means of exact diagonalization, and use the insights into the finite size effects to reconstruct the topological degeneracy in a small example system.

Keywords: solvable lattice models, finite-size scaling, other numerical approaches

J. Stat. Mech. (2009) P03006

Contents

1. Introduction

The Kitaev honeycomb model, first introduced in [1], is a system of spin-1/2 particles placed on the vertices of a hexagonal lattice. The system is known to exist in both Abelian and non-Abelian topological phases and is therefore relevant to on-going research into topologically fault-tolerant quantum information processing [2]–[4]. The system comprises two-body interactions and is exactly solvable in certain regimes, which makes it attractive both theoretically [5]–[18] and experimentally [19]–[22].

The presence of a topological phase implies the existence of anyons as quasi-particle excitations and it follows that the spectral properties, in particular ground state degeneracy, will depend dramatically on the topology of lattice [23]. In the Abelian phase for example, the low energy system can be mapped perturbatively in the fourth order onto the toric code Hamiltonian [1, 2]. The toric code system has a 4^g degenerate ground state where g is the genus of the surface. Recently (cf [12, 15, 18]), a more precise analysis of the planar system was given up to the tenth order of the perturbative expansion, while in [17] the exact form of the effective low energy Hamiltonian, valid on any torus, was derived. The latter analysis shows the precise order in the perturbative expansion at which the system topological degeneracy is broken but does not calculate the exact contributions of the finite size effects. In this paper, using Brillouin–Wigner perturbation theory, we calculate the finite size corrections associated with particular toroidal configurations of the honeycomb lattice, up to and including the fourth order. We demonstrate the accuracy of the perturbative method by comparison with exact numerical calculations. Finally, we use the obtained insights into the finite size effects to reconstruct the topological degeneracy in a small system.

doi:10.1088/1742-5468/2009/03/P03006

J. Stat. Mech. (2009) P03006

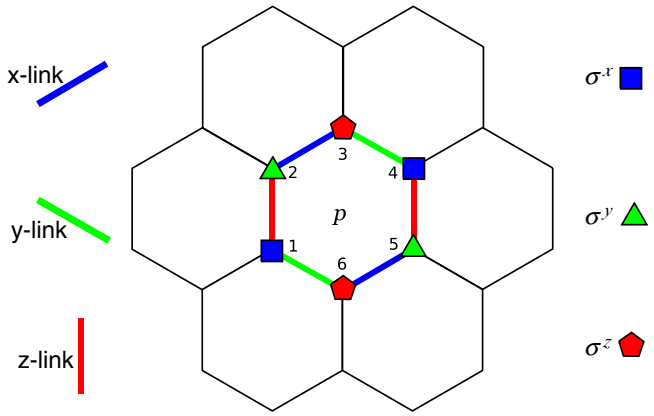

Figure 1. The honeycomb lattice and plaquette operator W_p.

1.1. The model

The Hamiltonian for the system can be written as

$$H = -\sum_{\alpha\in\{x,y,z\}}\sum_{i,j} J_\alpha K_{ij}^\alpha, \tag{1}$$

where $K_{ij}^\alpha \equiv \sigma_i^\alpha \otimes \sigma_j^\alpha$ denotes the exchange interaction occurring between the sites i, j connected by a α link; see figure 1. The plaquette operators

$$W_\mathrm{p} = \sigma_1^x\sigma_2^y\sigma_3^z\sigma_4^x\sigma_5^y\sigma_6^z, \tag{2}$$

where the numbers 1 through 6 label lattice sites on single hexagonal plaquette p (see figure 1), are the closed loop operators around each of the hexagons of the lattice. Since they commute with the Hamiltonian and with each other we may choose energy eigenvectors $|n\rangle$ such that $w_\mathrm{p} = \langle n\,|W_\mathrm{p}|n\rangle = \pm 1$. If $w_\mathrm{p} = -1$, one says that the state $|n\rangle$ carries a vortex at p.

The thermodynamic system is known to exist in four unique phases; see figure 2 and [1]. The three A phases are gapped and are related by permutations of x, y and z directions. The transition to the gapless B phase occurs when $J_\alpha = J_\beta + J_\gamma$. Note that this analysis applies only to the A phases of the system on a torus.

The lattice orientation in which we work is illustrated in figure 1. In order to specify a toroidal cell one need only specify two lattice vectors. The length of the vectors gives the periodicity in that direction, i.e. the start and end points of the vector specify the same point on the torus. In general we require a minimum periodicity of two hexagon cells along any direction. A more comprehensive classification of toroidal hexagonal tilings can be found in [27, 28].

One should be aware that, because of the periodic boundary conditions, certain seemingly different vector pairs can be used to describe the same torus tiling. Note also that a rotation of a particular lattice vector pair by $2n\pi/3$ or reflection about horizontal or vertical axis has the physical effect of permuting the values of J_x, J_y and J_z. Our convention therefore will be to fix one of the lattice vectors to $a\mathbf{i}$, where a is an integer. The other lattice vector may then be fixed to the positive quadrant without loss of generality. However, even with this convention there is still some redundancy in the definition and

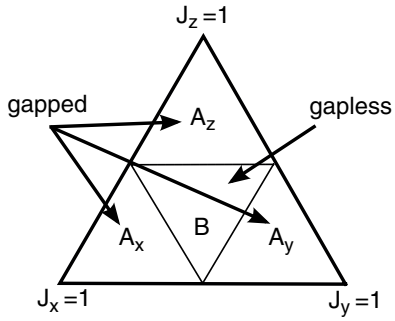

Figure 2. Visual representation of the system parameter space in the thermodynamic limit. The A phases are gapped. The B phase contains gapped vortices but gapless fermions [1].

some caution must be exercised. In figure 3 we illustrate some possible tilings and their associated lattice vectors.

2. The spectrum

The spectrum of any toroidal system depends a great deal on the underlying configuration. In the perturbative analysis of these configurations to follow we will in general see two forms for the non-finite size fourth-order effective Hamiltonian. These Hamiltonian are locally identical (i.e. are of the form $\sum Q_{\mathrm{p}}$) but have different topological degrees of freedom; see the appendix. The fourth-order non-finite size effective Hamiltonians that can be unitarily mapped to the toric code will be denoted as H_{K} (K for Kitaev) and those which cannot as H_{W} (W for Wen). In the table 1 we list the some of the possible small finite toric configurations and note the form of the non-finite size fourth-order contributions in each of the A phases.

We can now review the finite size corrections that enter the perturbative expansion for small toroidal configurations. It is a general property of the system that all terms in the effective Hamiltonian commute with each other. This means that eigenstates of the full effective Hamiltonian must also be eigenstates of the fourth-order effective system, although the reverse is not necessarily true. This does not of course imply that finite size effects have no effect on the eigenstates of the full system. In the appendix we will review the methodology used here and some of the relevant known results.

2.1. Second-order finite size corrections

In order to calculate the second-order corrections we see that, in almost all toroidal configurations, the only two term sequences that connect up basis elements of the dimerized subspace are those like $K^x_{ij}K^x_{ij}$ and $K^y_{ij}K^y_{ij}$. Since these terms connect each basis element to itself they are therefore constant [1]. However, in the $(a\mathbf{i}, 2\mathbf{j})$ configurations and the eight-spin $(2\mathbf{i}, 2\mathbf{n})$ configuration, because of the tight confinement, sequences like $K^x_{ij}K^y_{lm}$ and $K^y_{ij}K^x_{lm}$ can connect up different basis elements of the dimer subspace.

J. Stat. Mech. (2009) P03006

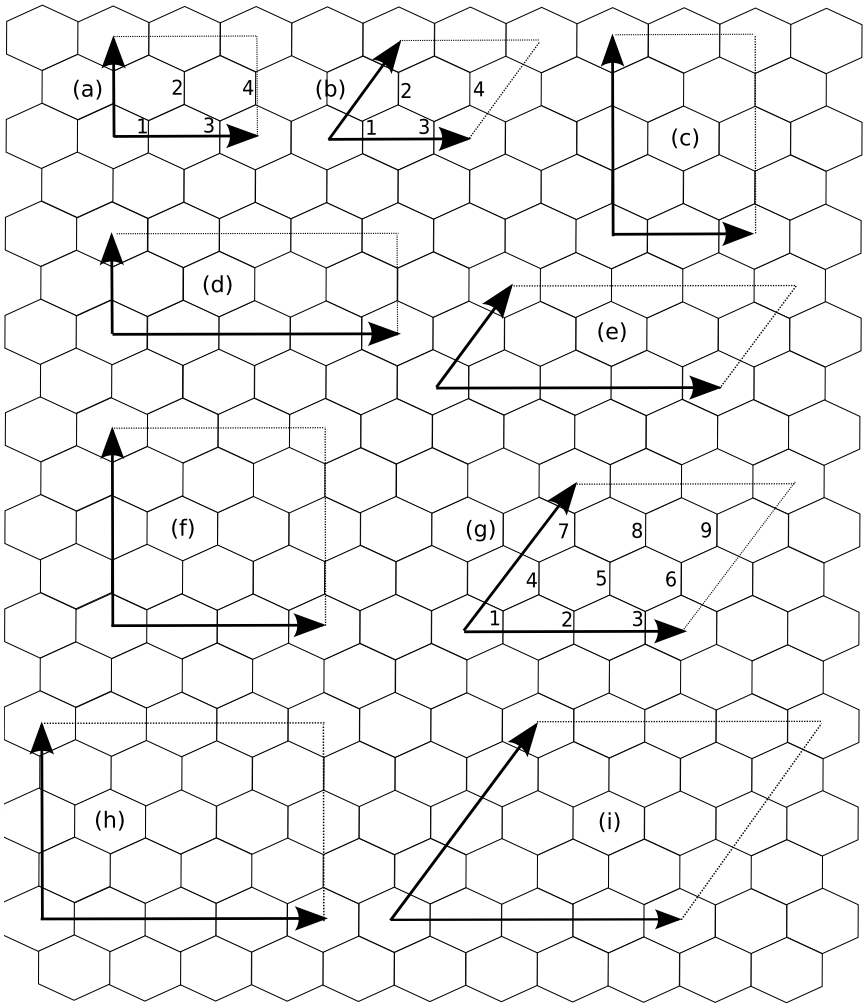

Figure 3. Some periodic configurations of the lattice. Each configuration is specified by two lattice vectors. Setting $\mathbf{n} = (\mathbf{i} + \sqrt{3}\mathbf{j})/2$ we see that configurations (a) $(2\mathbf{i}, 2\mathbf{j})$ and (b)$(2\mathbf{i}, 2\mathbf{n})$ contain 8 spins. (c) $(2\mathbf{i}, 4\mathbf{j})$, (d) $(4\mathbf{i}, 2\mathbf{j})$ and (e)$(4\mathbf{i}, 2\mathbf{n})$ are three 16-spin configurations. (f) $(3\mathbf{i}, 4\mathbf{j})$ is a 24-spin system and (g) $(3\mathbf{i}, 3\mathbf{n})$ is an 18-spin system, the only one depicted with an odd number of plaquettes. (h) $(4\mathbf{i}, 4\mathbf{j})$ and (i) $(4\mathbf{i}, 4\mathbf{n})$ are two possible 32-spin systems related to each other by a twist of the boundary conditions. Note that configurations (g) and (i) are the only configurations shown that are symmetric with respect to x, y and z links.

Using the rules given in (A.4) we see that in the $N = 8$ spin $(2\mathbf{i}, 2\mathbf{n})$ configuration the non-constant second-order effective Hamiltonian is

$$H^{(2)} = \frac{1}{2|J_z|}[J_x^2(\sigma_1^x\sigma_2^x + \sigma_3^x\sigma_4^x) + J_y^2(\sigma_2^x\sigma_3^x + \sigma_1^x\sigma_4^x)], \tag{3}$$

where the subscripts are shown in figure 3(b). For all $(a\mathbf{i}, 2\mathbf{j})$ configurations the spectral properties of the A_z phase are different from the A_x and A_y phases. In the A_z phase the

Table 1. List of toroidal configurations and type of fourth-order non-finite size Hamiltonian obtained in each A phase.

N	Configuration	A_x	A_y	A_z
8	$(2\mathbf{i}, 2\mathbf{j})$	H_{W}	H_{W}	H_{K}
8	$(2\mathbf{i}, 2\mathbf{n})$	H_{K}	H_{K}	H_{K}
12	$(3\mathbf{i}, 2\mathbf{j})$	H_{W}	H_{W}	H_{K}
12	$(3\mathbf{i}, 2\mathbf{n})$	H_{W}	H_{W}	H_{K}
16	$(2\mathbf{i}, 4\mathbf{j})$	H_{K}	H_{K}	H_{K}
16	$(4\mathbf{i}, 2\mathbf{j})$	H_{W}	H_{W}	H_{K}
16	$(4\mathbf{i}, 2\mathbf{n})$	H_{K}	H_{K}	H_{K}
18	$(3\mathbf{i}, 3\mathbf{n})$	H_{W}	H_{W}	H_{W}
20	$(5\mathbf{i}, 2\mathbf{j})$	H_{W}	H_{W}	H_{K}
20	$(5\mathbf{i}, 2\mathbf{n})$	H_{W}	H_{W}	H_{K}
24	$(2\mathbf{i}, 6\mathbf{j})$	H_{W}	H_{W}	H_{K}
24	$(3\mathbf{i}, 4\mathbf{j})$	H_{W}	H_{W}	H_{K}
24	$(6\mathbf{i}, 2\mathbf{j})$	H_{W}	H_{W}	H_{K}
24	$(6\mathbf{i}, 2\mathbf{n})$	H_{K}	H_{K}	H_{K}
28	$(5\mathbf{i}, 2\mathbf{j})$	H_{W}	H_{W}	H_{K}
28	$(5\mathbf{i}, 2\mathbf{n})$	H_{W}	H_{W}	H_{K}
30	$(3\mathbf{i}, 5\mathbf{n})$	H_{W}	H_{W}	H_{W}
32	$(2\mathbf{i}, 8\mathbf{j})$	H_{K}	H_{K}	H_{K}
32	$(4\mathbf{i}, 4\mathbf{j})$	H_{K}	H_{K}	H_{K}
32	$(4\mathbf{i}, 4\mathbf{n})$	H_{K}	H_{K}	H_{K}
32	$(8\mathbf{i}, 2\mathbf{j})$	H_{W}	H_{W}	H_{K}
32	$(8\mathbf{i}, 2\mathbf{n})$	H_{K}	H_{K}	H_{K}
36	$(3\mathbf{i}, 6\mathbf{j})$	H_{W}	H_{W}	H_{K}
50	$(5\mathbf{i}, 5\mathbf{n})$	H_{W}	H_{W}	H_{W}

second-order effective system is governed by a simple Ising spin chain Hamiltonian

$$H^{(2)} = \frac{1}{2|J_z|} J_x J_y \sum_{n=1}^{N/2} \sigma_n^y \sigma_{n+1}^y, \tag{4}$$

where the subscripts (see for example figure 3(a)) are modulo $N/2$.

2.2. Third-order corrections

To consider the third-order perturbation correction for finite systems we play an identical game except that this time we must consider weighted sums over terms like

$$\langle a\,|V|j\rangle\langle j\,|V|k\rangle\langle k\,|V|b\rangle. \tag{5}$$

This means that we need three term sequences, $K_{ij}^{\alpha} K_{lm}^{\beta} K_{no}^{\gamma}$, that connect up the dimerized basis elements $|a\rangle$ and $|b\rangle$. Sequences like this occur for example in the A_x and A_y phases of $(a\mathbf{i}, 2\mathbf{j})$ configurations with $a > 2$, and in all the A phases of the 18-spin $(3\mathbf{i}, 3\mathbf{n})$ configuration. This 18-spin system is unusual because the unit cell is 3×3 plaquettes and it cannot be mapped to the toric code in any of its A phases. However, for related reasons, there are no fourth-order finite size effects and therefore the only fourth-order terms are

doi:10.1088/1742-5468/2009/03/P03006

J. Stat. Mech. (2009) P03006

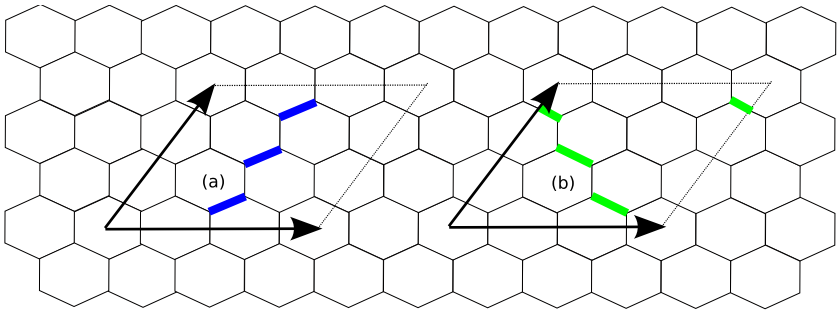

Figure 4. Graphical representations of two of the six third-order finite size corrections terms for the 18-spin $(3\mathbf{i}, 3\mathbf{n})$ configuration.

those related to the plaquette symmetries of (A.6). This means that, by first accounting for the third-order finite size effects, we can see the energy dependence on vorticity and ground state degeneracy predicted by [29] in the numerical calculations.

We illustrate two of the six third-order finite-size terms in figure 4. The full effective third-order Hamiltonian can be written as:

$$H^{(3)} = \frac{3}{8|J_z|^2}[J_x^3 \sum_{n=0}^{2} \sigma_{3n+1}^x \sigma_{3n+2}^x \sigma_{3n+3}^x - J_y^3 \sum_{n=0}^{2} \sigma_{n+1}^x \sigma_{n+4}^x \sigma_{n+7}^x], \tag{6}$$

where the numbering of the effective spins used is shown in figure 3(g). Setting $J = J_x = J_y$ gives a spectrum with 3 degenerate energy levels at

$$E^{(3)} = \begin{bmatrix} +\frac{3|J|^3}{2|J_z|^2} \\ 0 \\ -\frac{3|J|^3}{2|Jz|^2} \end{bmatrix}, \tag{7}$$

where the upper and lower splittings are 96 times degenerate and the 0 energy term is 320 times degenerate.

2.3. Fourth-order corrections

In this section we examine the additional finite size terms that appear in the fourth-order perturbative expansion. As an example we consider the 16-spin $(2\mathbf{i}, 4\mathbf{j})$ configuration in the A_z phase. This particular configuration is important in that all the alternative non-constant fourth-order terms are present in one form or another. In figure 5 we illustrate some of the ways that different basis elements are connected for the 16-spin $(2\mathbf{i}, 4\mathbf{j})$ configuration. The plaquette terms Q_p are of type (a). There are also 16 sequences that go around the torus in the 'vertical' direction and 12 that go in the 'horizontal' direction. The overall non-constant fourth-order effective Hamiltonian is therefore a quite complicated entity with a number of different excitation types; see figure 5.

The full fourth-order effective Hamiltonian for this configuration may be written as

$$H^{(4)} = -\frac{J_x^2 J_y^2}{16|J_z|^3} \sum_{n=1}^{8} (Q_n + R_n - 5A_n) - \frac{J_x^2 J_y^2}{16|J_z|^3} \sum_{n=1}^{4} (Z_n + 5Y_n) - \frac{5}{16|J_z|^3} \left(J_x^4 \sum_{n=1}^{2} X_n + J_y^4 \sum_{n=3}^{4} X_n \right), \tag{8}$$

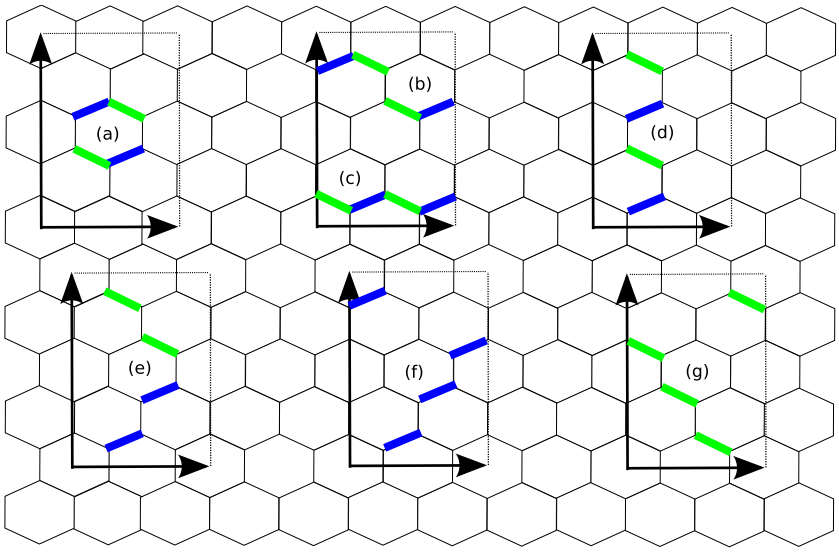

Figure 5. Some different four terms sequences that non-trivially connect up the dimer basis vectors on the 16-spin $(2\mathbf{i}, 4\mathbf{j})$ configuration lattice. Type (a) is a plaquette term Q_n and is valid for all non-horizontal configurations. Types (b) and (c) are horizontal string terms R_n and Z_n respectively. Type (d) and (e) are vertical strings Y_n and A_n respectively. Types (f) and (g) are vertical X_n strings.

where the R_ns are (horizontal) strings of the form $\sigma^z\sigma^x\sigma^z\sigma^x$, with the σ^xs operating on dimers that are acted on at both ends by a σ^x or σ^y in the full system. The horizontal Z terms contain four effective σ^z terms and the vertical X and Y strings contain four effective σ^xs and σ^ys respectively. The eight (vertical) A terms are mixtures of two effective σ^y and σ^x terms; see figure 5.

2.3.1. Case study: 24-spin $(3\mathbf{i}, 4\mathbf{j})$ *configuration.* As the system size is increased certain terms drop out of the fourth-order calculation. For example we can extend the 16-spin $(2\mathbf{i}, 4\mathbf{j})$ configuration to a 24-spin configuration in two different ways. Extending the system vertically to a $(2\mathbf{i}, 6\mathbf{j})$ configuration means taking the X, Y and A terms from the fourth-order calculation and adding in additional Z and R terms. If we extend the system horizontally, so that we have a $(3\mathbf{i}, 4\mathbf{j})$ plaquette configuration, all the Z, R and X terms drop out while additional Y and A 'vertical' terms must be added in.

In this case, if we set $J = J_x = J_y$, the full effective Hamiltonian can be written as

$$H_{\mathrm{eff}} = cI + J_{\mathrm{eff}}(H_{\mathrm{K}} + H_{\mathrm{FS}}^{(4)}) + \mathrm{O}(J^6), \tag{9}$$

where $J_{\mathrm{eff}} = J^4/(16|J_z|^3)$ and

$$H_{\mathrm{FS}}^{(4)} = -5\left(\sum_{n=1}^{6} Y_n - \sum_{n=1}^{12} A_n\right). \tag{10}$$

One way to demonstrate the accuracy of the above calculation is to subtract out the low order finite size contributions from the numerically calculated spectrum. This leaves the toric code contribution plus higher order corrections. First we define $\sigma(M)$ as the

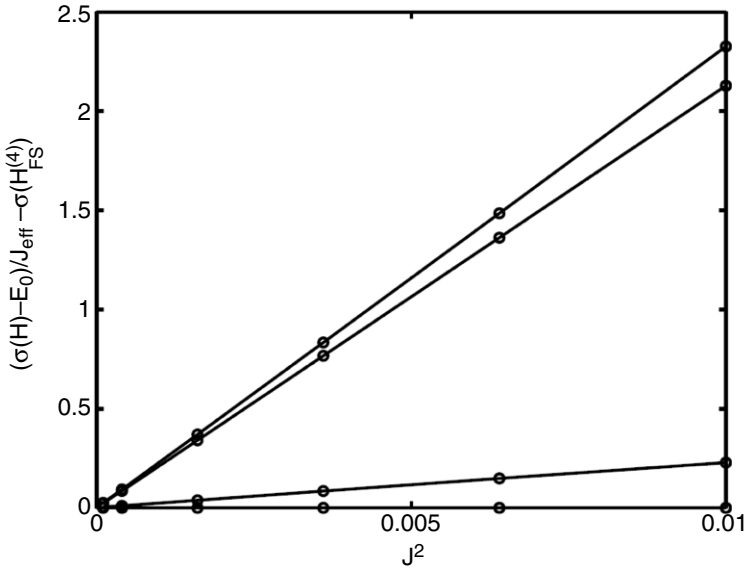

Figure 6. $(\sigma(H) - E_0)/J_{\rm eff} - \sigma(H^{(4)}_{\rm FS})$ versus J^2. Lifting of the $(3\mathbf{i}, 6\mathbf{j})$ toroidal honeycomb model ground state degeneracy via sixth-order finite size effects.

appropriately ordered spectrum of any operator M and then note that

$$\frac{\sigma(H) - E_0}{J_{\rm eff}} - \sigma(H^{(4)}_{\rm FS}) = \sigma(H_{\rm K}) + {\rm O}(J^2). \tag{11}$$

In figure 6 we plot the lowest four values of the lhs of this equation as a function of J^2. The splitting of the four-fold degenerate ground state due to the sixth-order finite size effects is clearly demonstrated.

2.4. Minimum valid toric code lattice

It is useful to ask in what configurations the perturbative expansion to the fourth-order term is equivalent to the toric code Hamiltonian. Using the arguments like those above we see that we can rule out all finite size terms at the fourth and lower orders in the A_z phase of the 30-spin $(3\mathbf{i}, 5\mathbf{n})$ configuration. However, the effective fourth-order Hamiltonian is not unitarily equivalent to the toric code and is of the type $H_{\rm W}$ in all A phases. However, the A_z phase of the 36-spin $(3\mathbf{i}, 6\mathbf{j})$ (or equivalently $(3\mathbf{i}, 6\mathbf{n})$) configuration has finite size effects on the terms of sixth order and above, and the fourth-order term can be unitarily mapped to the toric code.

It is interesting that this number of spins, 36, may also obtained by requiring that plaquette terms $Q_{\rm p}$ share only one effective spin. To satisfy this requirement we need a minimum of 18 effective spins. In figure 7 we plot this 36-spin configuration and its associated 18-spin toric code lattice.

3. Conclusion

In this paper we first reviewed the toroidal configurations of the honeycomb lattices. We then listed of some of the smaller configurations and the properties of their non-finite size

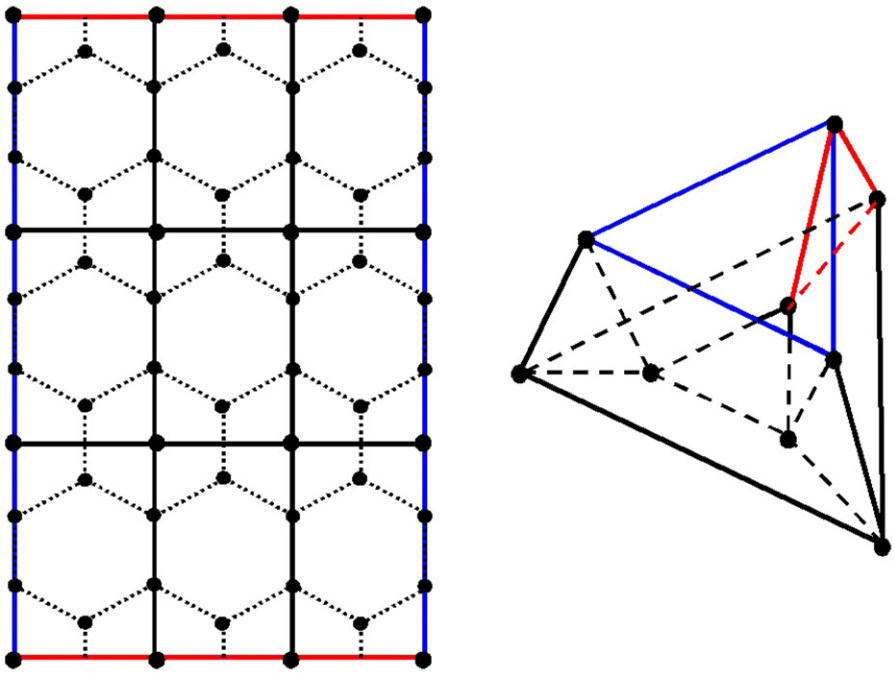

Figure 7. The 36-spin $(3\mathbf{i}, 6\mathbf{j})$ configuration with and its associated toric code lattice.

fourth-order effective Hamiltonian in each A phase. Typical examples of second-, third- and fourth-order finite size effects were given for a number of different configurations. We noted that a minimum of 36 spins in the full system are needed for the fourth-order effective Hamiltonian to be equivalent to the Kitaev's toric code. We confirmed, by exact diagonalization of a 24-spin Hamiltonian, the accuracy of the methodology.

Acknowledgments

The authors wish to acknowledge Science Foundation Ireland (SFI) for financial support through the President of Ireland Young Researcher Award, and the SFI/HEA Irish Centre for High-End Computing (ICHEC) for the provision of computational facilities and support. The authors thank to Tim Stitt and Joost Slingerland for discussions.

Appendix. Mapping to the toric code

The spectrum of the system can be given a simple description when two of the parameters J_x, J_y or J_z are zero (the corners of the phase diagram). In this case we can think of the system as $N/2$ non-interacting dimers and the spectrum of the system consists of $N/2+1$ levels. The lowest level has an energy of $J_r N/2$ where J_r is either J_x, J_y or J_z and the gap between successive levels is $2J_r$. The degeneracy of the nth-lowest level is given by

$$d(n) = 2^{N/2} \binom{N/2}{n-1}. \tag{A.1}$$

Following Kitaev we take $J_z \gg J_x, J_y$ and write the Hamiltonian as $H = H_0 + U$, where $H_0 = -J_z \sum_{ij} K_{ij}^z$ is the unperturbed Hamiltonian and $U = -\sum_{\alpha\in\{x,y\}} J_\alpha \sum_{ij} K_{ij}^\alpha$ is the

perturbative contribution. H_0 has a $2^{N/2}$-fold-degenerate ground state space spanned by ferromagnetic configurations of the dimers on z links. To understand how this degeneracy behaves under perturbation we analyze the Brillouin–Wigner expansion [24, 25]. The method returns the systems energies E as an implicit non-linear eigenvalue problem and thus, for the actual calculation of coefficients to high orders, can be difficult to apply [26].

Define $\mathcal{P}$ to be the projector onto this ferromagnetic subspace and note that for any exact eigenstate of the full Hamiltonian $|\psi\rangle$, its projection $|\psi_0\rangle$ onto the subspace satisfies

$$\left[E_0 + \sum_{n=1}^{\infty} H^{(n)}\right] |\psi_0\rangle = E|\psi_0\rangle = H_{\text{eff}}|\psi_0\rangle, \tag{A.2}$$

where $H^{(n)} = \mathcal{P}U\mathcal{G}^{n-1}\mathcal{P}$, $\mathcal{G} = [1/(E - H_0)](1-\mathcal{P})U$ and E_0 is the ground state energy of H_0. The eigenstates, with eigenvalue E, of the effective system and full system are related by the expression $|\psi\rangle = (1-\mathcal{G})^{-1}|\psi_0\rangle = \sum_{n=0}^{\infty}\mathcal{G}^n|\psi_0\rangle$.

For our purposes we rewrite this method using the dimerized basis as our effective basis and calculate the non-constant perturbation corrections as

$$\begin{aligned}
\langle a\,|H^{(1)}|b\rangle &= \langle a\,|V|b\rangle = 0,\\
\langle a\,|H^{(2)}|b\rangle &= \sum_{j} \frac{\langle a\,|V|j\rangle\langle j\,|V|b\rangle}{E_0 - E_j},\\
\langle a\,|H^{(3)}|b\rangle &= \sum_{jk} \frac{\langle a\,|V|j\rangle\langle j\,|V|k\rangle\langle k\,|V|b\rangle}{(E_0 - E_j)(E_0 - E_k)},\\
\langle a\,|H^{(4)}|b\rangle &= \sum_{jkl} \frac{\langle a\,|V|j\rangle\langle j\,|V|k\rangle\langle k\,|V|l\rangle\langle l\,|V|b\rangle}{(E_0 - E_j)(E_0 - E_k)(E_0 - E_l)},
\end{aligned} \tag{A.3}$$

where $|a\rangle$ and $|b\rangle$ $(a \neq b)$ are basis vectors of the dimerized Hilbert space and states $|j\rangle, |k\rangle$ and $|l\rangle$ are higher energy states orthogonal to the ground state manifold. Here the unperturbed eigenvalues E_0 are used to calculate the denominator. This approximation ultimately means that the method is accurate only for non-constant, low order coefficients of the effective Hamiltonian [24]–[26].

To find the nth-order non-constant correction we need to find the non-zero elements of the matrix $H^{(n)}$. This is done by finding all the (length n) sequences of terms $K_{ij}^{a^{(1)}}, \ldots, K_{lm}^{a^{(n)}}$ with $a^{(m)} \in x, y$ that connect different basis elements of the dimerized subspace. The resulting low energy effective Hamiltonian can be written in terms of operators acting on the spins of the dimers using the following transformation rules:

$$\begin{aligned}
&\mathcal{P}[\sigma^x \otimes \sigma^y] \to +\sigma^y, \qquad &&\mathcal{P}[\sigma^x \otimes \sigma^x] \to +\sigma^x,\\
&\mathcal{P}[\sigma^y \otimes \sigma^y] \to -\sigma^x, \qquad &&\mathcal{P}[\sigma^z \otimes I] \to +\sigma^z,\\
&\mathcal{P}[\sigma^z \otimes \sigma^z] \to +I,
\end{aligned} \tag{A.4}$$

where the right-hand side is now a representation of the effective spin operation. The effective Hilbert space now consists of $M = N/2$ effective spins. The effective σ^z terms occur when we have a sequence that contains a K_{ij}^x and a K_{jk}^y term. In this case it is important to note that the order of the sequence determines a sign factor which must be accounted for when summing over the total combinations.

J. Stat. Mech. (2009) P03006

By analyzing all possible loop symmetries of the full system on a torus it was shown that the effective Hamiltonian must be of the following form (cf [17]):

$$H_{\text{eff}} = \sum_{k=0}^{3} \sum_{l=1}^{2^{N/2-2}} d_{k,l} G_k(z,y) F_l(Q_1, Q_2, \ldots, Q_{N/2-2}). \tag{A.5}$$

Here $G_0 = I$, $G_1 = z$, $G_2 = y$ and $G_3 = zy$ where z and y are both homologically non-trivial sequences $K_{ij}^{a^{(1)}}, \ldots, K_{lm}^{a^{(n)}}$ with $a^{(m)} \in x, y$ and from different homological classes. The $d_{k,l}$ are coefficients which depend on J_x, J_y and J_z.

In the thermodynamic limit Kitaev showed that all first-and third-order coefficients are zero. The first non-constant term, occurring at the fourth order, was calculated to be

$$H^{(4)} = -\frac{J_x^2 J_y^2}{16|J_z|^3} \sum Q_{\text{p}}, \tag{A.6}$$

where $Q_{\text{p}} = \sigma_l^y \sigma_d^z \sigma_r^y \sigma_u^z$ are the effective spin representations of the operator W_{p} in equation (2) [1]. The subscripts in this notation denote the relative position of the site on each plaquette (left, down, right, up). Calculations of the planar effective Hamiltonian of up to the tenth order have been recently obtained [12, 15, 18].

The spectrum of the fourth-order effective system depends both the underlying lattice configuration and which the A phase is under consideration. If the square toroidal lattice of the effective system can be bi-colored it has two non-trivial relations $\prod Q_b = I$ and $\prod Q_w = I$ and is unitarily equivalent to the toric code [1]. If the square lattice cannot be bi-colored it has only one non-trivial relation $\prod Q_{\text{p}} = I$ and is only twofold degenerate [29].

References

[1] Kitaev A, 2006 *Ann. Phys.* **321** 2
[2] Kitaev A, 2003 *Ann. Phys.* **303** 2
[3] Pachos J K, 2006 *Int. J. Quant. Inf.* **4** 947
[4] Nayak C *et al*, 2008 *Rev. Mod. Phys.* **80** 1083
[5] Pachos J K, 2007 *Ann. Phys.* **322** 1254
[6] Zhang C *et al*, 2007 *Proc. Nat. Acad. Sci.* **104** 18415
[7] Chen H-D and Hu J, 2007 *Phys. Rev.* B **76** 193101
[8] Chen H-D and Nussinov Z, 2008 *J. Phys. A: Math. Theor.* **41** 075001
[9] Baskaran G *et al*, 2007 *Phys. Rev. Lett.* **98** 247201
[10] Lahtinen V *et al*, 2008 *Ann. Phys.* **323** 9
[11] Feng X-Y *et al*, 2007 *Phys. Rev. Lett.* **98** 087204
[12] Schmidt K P *et al*, 2008 *Phys. Rev. Lett.* **100** 057208
[13] Vidal J *et al*, 2008 arXiv:0801.4620
[14] Zhang C *et al*, 2008 arXiv:0801.4918
[15] Dusuel S *et al*, 2008 *Phys. Rev. Lett.* **100** 177204
[16] Wootton J R *et al*, 2008 *Phys. Rev.* B **78** 161102(R)
[17] Kells G *et al*, 2008 *Phys. Rev. Lett.* **101** 240404
[18] Vidal J *et al*, 2008 arXiv:0809.1553
[19] Duan L M *et al*, 2003 *Phys. Rev. Lett.* **91** 090402
[20] Micheli A *et al*, 2006 *Nat. Phys.* **2** 341
[21] Jiang L *et al*, 2007 arXiv:0711.1365
[22] Aguado M *et al*, 2008 arXiv:0802.3163
[23] Einarsson T, 1990 *Phys. Rev. Lett.* **64** 1995
[24] Ziman J M, 1969 *Elements of Advanced Quantum Theory* (Cambridge: Cambridge University Press)
[25] Killingbeck J, 1977 *Rep. Prog. Phys.* **40** 963
[26] Bergman D L *et al*, 2007 *Phys. Rev.* B **75** 094403

J. Stat. Mech. (2009) P03006

[27] Kirby E C *et al*, 1993 *J. Chem. Soc. Faraday Trans.* **89** 1945
[28] László I *et al*, 2001 *Chem. Phys. Lett.* **342** 369
[29] Wen X-G, 2003 *Phys. Rev. Lett.* **90** 016803